Chaotic Properties of Hemodynamic Response in Functional Near Infrared Spectroscopic Measurement of Brain Activity

Ni Ni Soe , Masahiro Nakagawa

Abstract—Functional near infrared spectroscopy (fNIRS) is a practical non-invasive optical technique to detect characteristic of hemoglobin density dynamics response during functional activation of the cerebral cortex. In this paper, fNIRS measurements were made in the area of motor cortex from C4 position according to international 10-20 system. Three subjects, aged 23 - 30 years, were participated in the experiment.

The aim of this paper was to evaluate the effects of different motor activation tasks of the hemoglobin density dynamics of fNIRS signal. The chaotic concept based on deterministic dynamics is an important feature in biological signal analysis. This paper employs the chaotic properties which is a novel method of nonlinear analysis, to analyze and to quantify the chaotic property in the time series of the hemoglobin dynamics of the various motor imagery tasks of fNIRS signal. Usually, hemoglobin density in the human brain cortex is found to change slowly in time. An inevitable noise caused by various factors is to be included in a signal. So, principle component analysis method (PCA) is utilized to remove high frequency component. The phase pace is reconstructed and evaluated the Lyapunov spectrum, and Lyapunov dimensions. From the experimental results, it can be conclude that the signals measured by fNIRS are chaotic.

Keywords—Chaos, hemoglobin, Lyapunov spectrum, motor imagery, near infrared spectroscopy (NIRS), principal component analysis (PCA).

I. INTRODUCTION

RECENTLY, a variety of non- invasive techniques have been adopted for measuring brain activity by means of not only electrical signal but also changes in cerebral hemodynamic and oxygenation. For electrical signal, electroencephalography (EEG) is very popular technique and positron emission tomography (PET), magneto encephalography (MEG), or functional magnetic resonance imaging (fMRI) has been used to measure changes in regional cerebral blood flow (CBF). These methods for CBF are expensive, not widely available, associated with injection of radioactive compounds, and have a low temporal resolution.

Near infrared spectroscopy (NIRS) and functional magnetic resonance imaging (fMRI) are rapidly developing technologies that both allow non-invasive monitoring of regional changes in cortical tissue oxygenation, particularly changes in deoxyhemoglobin concentration ([Hb]), in response to various stimuli including visual, auditory, and motor stimuli [9]-[10].

NIRS is a simple, in expensive and a new noninvasive optical technique, measures changes in concentrations of oxygenated and deoxygenated hemoglobin (oxy-Hb and deoxy-Hb, respectively) mainly in cerebral venous blood. Summation of the changes in oxy-Hb and deoxy-Hb indicates changes in the total hemoglobin concentration (total-Hb). The NIRS method is based on near-infrared light absorption changes that depend on concentration changes of the chromophores $[HbO_2]$ and $[Hb]$ in the tissue under investigation. Changes in [total-Hb] can be used as a measure of blood volume changes. NIRS promises flexibility of use, portability, metabolic specificity, good spatial resolution, localized information, high sensitivity in detecting small substance concentrations and affordability. NIRS has no doubt certain disadvantages. It is slow to operate because of the inherent latency of the hemodynamic response. The signal strength is affected by hair on the head. Furthermore, relative motion of the optodes on the hair may introduce motion artifacts and drifts in the hemodynamic signal. Nevertheless, NIRS' ability to record localized brain activity with a spatial resolution in the order of centimeter (depending on the probe geometry) provides with an excellent opportunity to control a variety of motor and cognitive activities. Actually, there have been many research areas on NIRS not only in brain but also in pharmaceutical, Agricultural application and so on [11].

According to the brain activity research, many researchers have been analyzed fNIRS signals on cognition tasks [12], infant brain development [13], and spectral analysis of event related of fNIRS [14]. fNIRS was used also in the study of human cortical taste cognitive processing [15]. Sitaram et al. [16] and Coyle et al. [17] reported optical response using NIRS signals during overt and covert hand movements. For BCI application, motor tasks such as left hand, right hand imagery are common tasks [16]-[18]. D. Friedman et al. reported a direct EEG-based BCI using motor imagery [19]. It is important that, for a BCI to be user-friendly, the mental task should be easy to learn. With this view and based on the above findings, motor imagery tasks were chosen as the basis for the experiments. Information about peoples' current activity and their mental tasks can be used for multiple applications not only in healthy person but also in patients. This paper demonstrates the new application of chaos analysis on NIRS signal.

The authors are with the Chaos and Fractals Informatics Laboratory (NLAB), Department of Electrical Engineering, Faculty of Engineering, Nagaoka University of Technology, 1603-1 Kamitomioka, Nagaoka, Niigata 940-2188 Japan. TEL: +81-2-5847-1611 (ext. 5146); FAX: +81-258-47-9500; E-mail: ninisoe@pelican.nagaokaut.ac.jp

World Academy of Science, Engineering and Technology
International Journal of Psychological and Behavioral Sciences
Vol:2, No:3, 2008

Chaos analysis, such as the embedding theorem, the mutual information method, false nearest neighboring method, the largest Lyapunov exponent and so on, is a powerful non-linear method [20] which enables the extraction of characteristic quantities. It offers tools that bridge the gap between experimentally observed irregular behavior and deterministic chaos theory [21]–[28]. The interest in chaotic research has risen rapidly and several attempts have been made in many related fields such as mathematics, physics, chemistry and biomedical engineering as well as applications to the human brain and heart [3], [5], [6].

The aim of this paper is to investigate the chaotic property of hemoglobin changes of the blood within motor cortex by Lyapunov analysis. Lyapunov exponents of a given time series are of grate importance. Motor imagery of left-hand, and relax condition were chosen as the tasks as it has been shown to work well in previous research on EEG based fractal analysis [3]-[4]. To verify the chaotic property of NIRS signal, the real movement of motor cortex was also analyzed. This is the first time that Lyapunov exponent analysis has been used to NIRS signal to the best of our knowledge.

In this paper, it was described that the experimental paradigm of motor imagery; method of signal acquisition; preliminary signal analysis for artifact removal technique by PCA in the hemodynamic response to motor imagery; chaotic analysis of the NIRS signal using reconstruction of the attractor and Lyapunov spectrum; and finally the results of signal processing and analysis. Lyapunov spectrum was analyzed not only for forward time series of NIRS signal but also for reverse time series of NIRS signal to validate the Lyapunov exponents. This paper was concluded with a discussion of the application of these techniques to the classification problem towards developing a NIRS–BCI system by time dependent Lyapunov spectrum and fractal dimension.

II. MATERIALS AND METHODS

A. Subjects and motor imagery tasks

Three subjects with the age ranging from 23 years and 30 years voluntarily participated in this study. None of the recruited subjects had neurological or psychiatric history or was on medication.

Motor imagery is described as the mental rehearsal of a motor act without any overt motor output [1]. Mental imagination of movements involves similar brain regions that are used in programming and preparing movements. According to this view, the main difference between motor performance and motor imagery is that in the latter case execution would be blocked at some corticospinal level. Motor imagery, defined as mental simulation of a movement, has been shown to represent an efficient mental strategy [2]-[5]. The imagination of different types of movements, for example, right hand, left hand, or foot movement, results in a characteristic change of the hemoglobin density in the blood of the brain by fNIRS over the sensorimotor cortex of a participant. So, in this work, the motor imagery tasks were chosen for the experiments.

B. Experimental setup

During the experiment, the subjects were seated in a position that allowed them to perform the task comfortably. The subjects were asked to maintain a stable body position and avoid eye blinks, teeth bites and head movements during
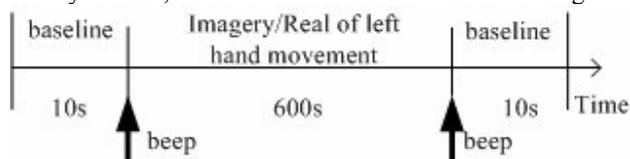
(a) Experimental protocol
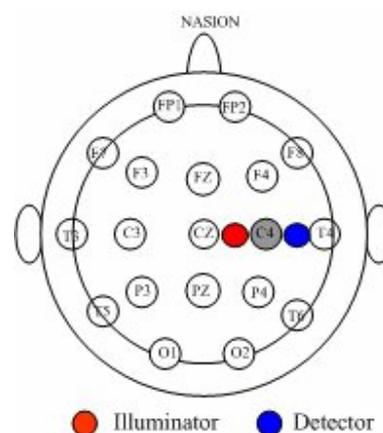
(b) The placement of NIRS optodes position on the scalp according to international 10-20 system.

Fig.1 (a) Experimental paradigm for imagery movement and (b) NIRS optodes position on the scalp. A pair of illuminators and detectors formed one channel.

the recording. Possible sources of distraction or noise, such as sound or light, were minimized. NIRS signals were recorded from each subject performing relax, real and imagery movements of left hand movement sequentially. Fig. 1(a) shows the schematic diagram of the protocol. At each task, the subjects performed 3 trials and each for duration of total 620 seconds. A single trial comprised of a baseline block, a preparation block and a motor task block. Each trial started and ended with a baseline block during which the subject fixated on the cross displayed on the screen for 20s. This was followed by a beep indicating the subject to get ready for the motor task. Following this, the subject performed the motor task as indicated on the screen for a period of 600 s. The type of motor task to be performed was instructed by the operator such as "Please imagine left hand movement".

Between any two adjacent trials, the subjects had sufficient relax so that the effect of muscle fatigue was minimized. Time gap of 20 minutes is given between any two successive tasks to ensure that a previous state stimulus doesn't affect the subsequent state of NIRS signal.

C. fNIRS signal acquisition

A multichannel fNIRS instrument (OMM-3000 from Shimadzu Corporation, Japan) for acquiring oxygenated hemoglobin and deoxygenated hemoglobin concentration

World Academy of Science, Engineering and Technology
International Journal of Psychological and Behavioral Sciences
Vol:2, No:3, 2008

changes during motor imagery. The system operated at three different wavelengths of 780 nm, 805 nm and 830 nm. The illuminator and detector optodes were placed on the scalp. The detector optodes were fixed at a distance of 3 cm from the illuminator optodes. The optodes were placed over the motor cortex at the position of C4 according to the 10 to 20 system for standard electrode positions (American Electroencephalographic Society, 1994). A pair of illuminator and detector optodes formed one channel on sensorimotor cortex was shown in the Fig. 1(b). Near-infrared rays leave illuminator, pass through the skull and the brain tissue of the cortex and are received by the detector optodes.

The photomultiplier cycles through all the illuminator–detector pairings to acquire data at every sampling period. The optodes were attached to a tight elastic headband in order to press them against the scalp. Changes in total-Hb, oxy-Hb, and deoxy-Hb were sampled every 0.025 s and stored on a floppy disk for offline analysis by a computerized system.

It is also important to maintain a good connection with the scalp and also to push hair aside. Dark hair obstructing the photon's path can significantly attenuate the signal, and every effort must be made to overcome this problem; combing hair out of the way, fixing with hair gel and hair clips are an imperative part of the experimental regime. A stable connection between the optodes and scalp is vital to ensure that the path length of the photons does not change and also to prevent ambient light saturating the detector. Before the beginning of the protocol, the oxygenation response was checked. If no oxygenation change could be detected, the optodes were replaced until a response was signaled. Example of oxy-Hb, deoxy-Hb, and total -Hb density changes for the dynamics of brain oscillations, of left hand motor imagery are presented in Fig. 2 (a-c).
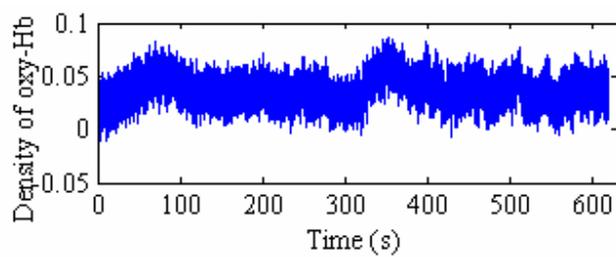
(a)
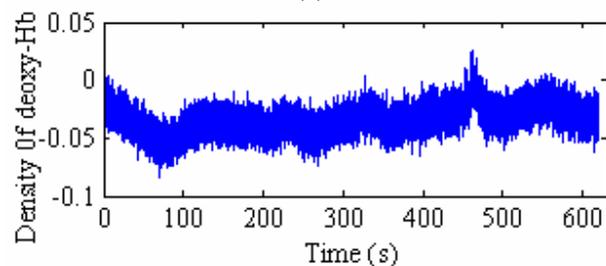
(b)
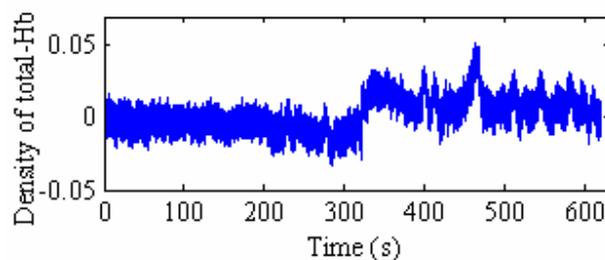
(c)

Fig. 2 The example of NIRS signal of imagery of left hand movement

D. Preprocessing by PCA

In many NIRS signal processing applications a sensor signal is contaminated with artifact and noise. The former sometimes can be the most prominent signal component registered, while the latter is often assumed to be additive, white, normally distributed and non-correlated with the sensor signals. Hence to recover the signals of interest, the task is to remove both the artifact and noise contributions. There is a wide range of noise-reduction tools is available. Together, they allow high quality measurements of brain activity. Nevertheless, some have drawbacks that interfere with the observation of brain response morphology. For others, prior removal of environmental noise would allow them to be optimized for the purpose of brain source analysis. In case the artifacts dominate, the useful signal can easily be extracted with projective subspace techniques such as principal component analysis (PCA) algorithm to get rid of most of the noise contributions to multidimensional signals [40].

The PCA method actually consists of three disjoint steps: Computing the principal components, projecting the data to obtain a low-dimensional representation, and reconstructing the cleaned data set. But many NIRS signals represent one dimensional time series. Clearly projective subspace techniques are not available for one dimensional time series to suppress noise contributions, hence time series analysis techniques often rely on embedding a one dimensional sensor signal in a high-dimensional space of time delayed coordinates [29]. So, NIRS signals on each channel which represent one dimensional time series need to be transformed to multidimensional signal vectors for the latter techniques to be applicable before computing the principal components. The transformation can be achieved by embedding an observed signal in its delayed coordinates. The time embedding of the signals transforms one dimensional time series into multidimensional signal vectors. This is a necessary step to have subspace projection techniques available. However, this step unavoidably introduces nonlinearity into the signal analysis process. For the observed one dimensional time series, x = $(x_1, x_2 ... x_N)$ can transform to a multidimensional sequence of $M = N-(m-1)\tau_d$ by time lag τ_d and embedding dimension m [§. E]. The legged vectors then constitute the column of the trajectory matrix $\mathbf{X_i} = [x_i, \; x_{i+\tau}, ... , \; x_{i+(m-1)\tau_d}]$, i = 1, 2, …,M. Further processing of the data matrix is performed by PCA. It encompasses the following steps: After embedding, the data

World Academy of Science, Engineering and Technology
International Journal of Psychological and Behavioral Sciences
Vol:2, No:3, 2008

points $X_1,...,X_M \in \mathbf{R^m}$, of the trajectory matrix are computed the mean value;

$$\overline{X} = \frac{1}{M} \sum_{i=1}^{M} X_i . \tag{1}$$

A covariance matrix is computed in each column using zero mean data;

$$X_c = \frac{1}{M} \sum_{i=1}^{M} (X_i - \overline{X})(X_i - \overline{X})^{\mathrm{T}} . \tag{2}$$

Compute the eigenvectors, $u_1, u_2, ..., u_m \in \mathbf{R^m}$ and eigenvalue, $\lambda_1, \lambda_2, ..., \lambda_m \in \mathbf{R}$ of the covariance matrix is computed;

$$C = \langle X_c X_c^T \rangle = UDU^T . \tag{3}$$

The most popular scheme for simultaneously approximating all the eigenvalues of a matrix A is the remarkable QR algorithm. Afterwards denoising can be achieved by projecting the multidimensional signal into the subspace spanned by the eigenvectors corresponding to the largest eigenvalues. The eigenvectors with the largest eigenvalues correspond to the dimensions that have the strongest correlation in the data set.

Project the multidimensional signal to low- dimensional subspace, then the transformed data points is:

$$X_i' = \sum_{i=1}^{d} u_i X_i . \tag{4}$$

To decide the principal component in reduction of the signal, the Scree method was utilized.

Finally, the denoised data points can be reconstructed from the transformed data points:

$$X_i'' = \sum_{j=1}^{d} u_j \left[X_i' \right]_j \tag{5}$$

and the noise-reduced one dimensional signal, x, is then obtained by reverting the embedding.

Eigenvalue is calculated for the signal shown in Fig 2. These are plotted in descending order are shown in Fig 3. As shown in Fig 3, by using the largest eigenvalue, the reconstructed signal by PCA were shown in Fig 4 (a)-(c). As shown in Fig 4, it can be verified that the high frequency component of the signal is excluded in comparison with the observation signal in Fig 2 (a)-(c).
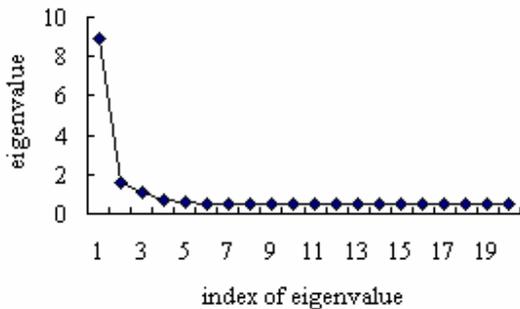

Fig. 3 The Scree plot of the eigenvalue in descending order of oxy-Hb density of Fig. 2(a)

E. Reconstruction of attractor

The first step is to reconstruct attractors from NIRS signals to apply chaos theory in NIRS analysis in a multidimensional phase space from a single time series. For this purpose, Takens' embedding theorem is used in this study and the trajectory of the attractor is reconstructed using the specified time delay from the time series [29]. Taking the signal on the given channel in a time series representation, NIRS data was recorded as a discrete time series $(x_1, x_2 ... x_N)$, where x is the signal amplitude at the discrete time moment N. The m-dimensional phase space is reconstructed from a single observable x_N by means of time delay method. The reconstructed trajectory, X, can be expressed as a matrix where each row is a phase-space vector. That is,

$$\mathbf{X} = [\mathbf{X}_1 \ \mathbf{X}_2 \ ... \mathbf{X}_M]^T \tag{6}$$
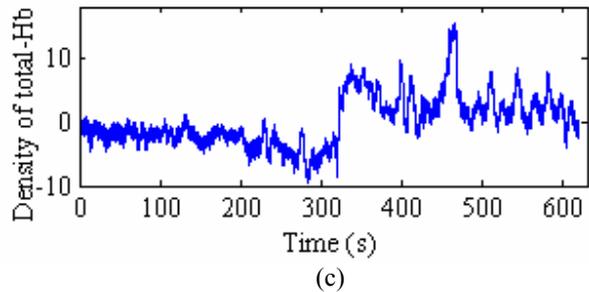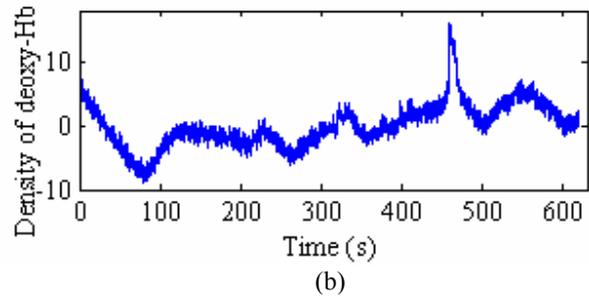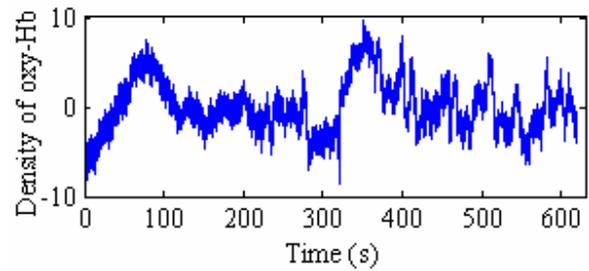

(a)

(b)

(c)

Fig. 4 The reconstructed signal of Fig 2 (a)-(c) by PCA

Where X_i is the state vector of the system at discrete time i. For an N-point time series, $\{x_1, x_2, x_N\}$, each X_i is given by:

$$\mathbf{X_i} = [x_i, \ x_{i+\tau}, ... , \ x_{i+(m-1)\tau_d}] . \tag{7}$$

Where τ_d is the *lag* or *reconstruction delay*, and m is the *embedding dimension*. Thus, X is an $M \times m$ matrix, and the constants $m, M, \tau_d,$ and N are related as:

$$M = N - (m-1)\tau_d \tag{8}$$

For an infinite amount of noise-free data, the quality of the reconstructed attractor, which will affect significantly the

World Academy of Science, Engineering and Technology
International Journal of Psychological and Behavioral Sciences
Vol:2, No:3, 2008

measurement of the dynamical invariants, depends on the value of chosen the time delay τ_d.

In this work, the time delayed mutual information which was suggested by Fraser and Swinney [30], is applied to determine a reasonable delay. Delay time (τ_d) determined based on the first local minimum in average mutual information function of the time series data x_i ($i = 1, 2… M$). At first, the sequence X_i ($i = 1, 2... M$), of length M is considered in the time series X_i. Second, by shifting the X_i by α, the new sequence of Y_j ($j = \alpha, \alpha+ 1… \alpha+M$). Let the probability distribution in $X_i = p_x$ (i) and the probability distribution in $Y_j = p_y$ (j). Then, the mutual information is:

$$I\,(X,Y) \;=\; \sum_i \sum_j p_{xy}(i,j)\, \log \frac{p_{xy}(i,j)}{p_x(i)p_y(j)} \qquad (9)$$

By varying the time shift α, let the time delay, for which $I(X, Y)$ first takes the local minimum, be the delay τ_d.

To determine the appropriate embedding dimension m of the reconstructed attractor, false nearest neighbour (FNN) method [31] was utilized. This method can yield an acceptable minimum embedding dimension by examining the behavior of nearest neighbors as the embedding dimension is increased from m to $m +1$. The result of time delay estimation of the given NIRS signal is shown in Fig. 5. Fig. 6 shows the fraction of false nearest neighbors for m on the attractors reconstructed from the NIRSl signals. One may find that the fraction of NIRS signals become zero for $m \geq 5$, which indicates an acceptable embedding dimension. So, $m = 5$ was used in the following Lyapunov analysis. The phase space plot for imagery of left hand movement NIRS signals after PCA analysis were shown in Fig. 7 and τ_d and m were selected according to the mutual information and false nearest neighboring results of Fig. 5 and Fig. 6.
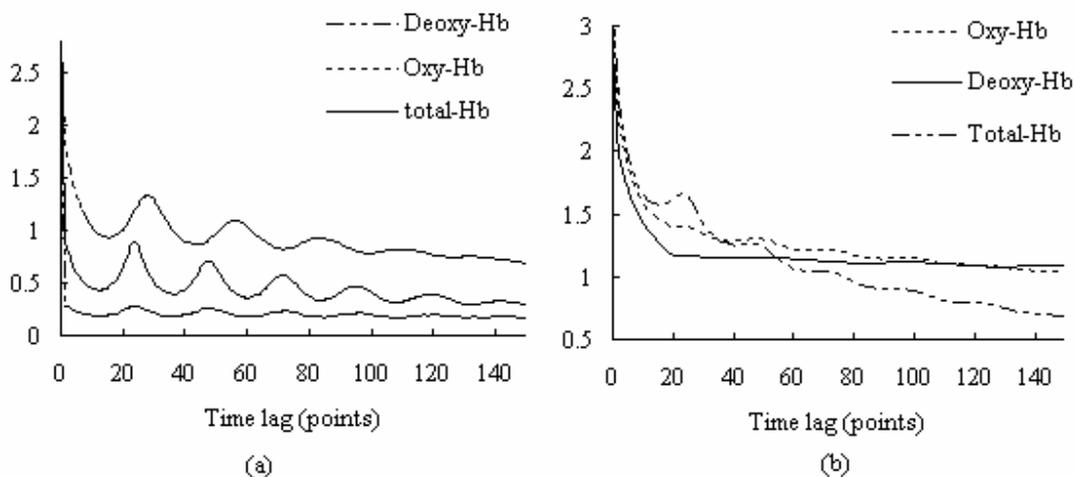

Fig. 5 Approximation to the mutual information of (a) original NIRS signals of Fig. 2(a)-(c) and (b) PCA applied NIRS signal Fig. 4(a)-(c)
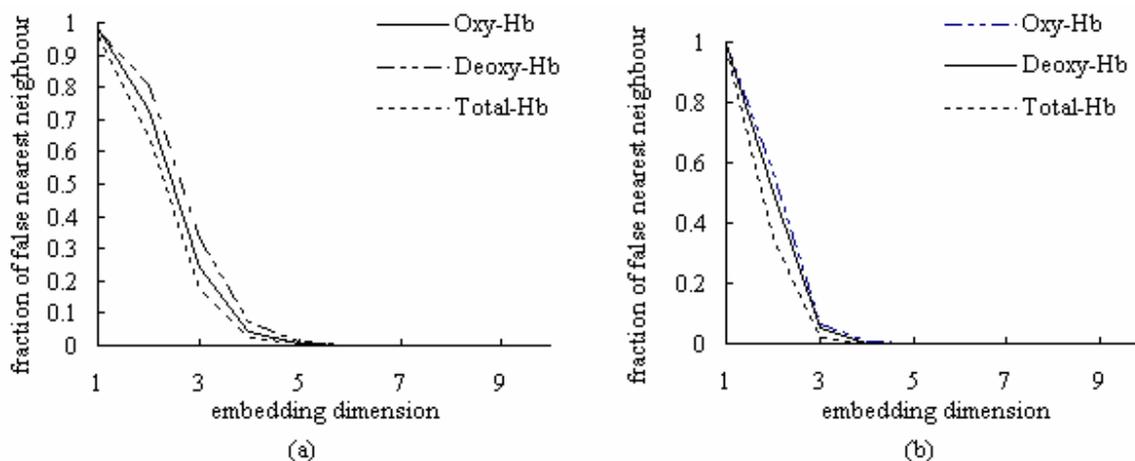

Fig. 6 Approximation to the embedding of (a) original NIRS signals of Fig. 2(a)-(c) and (b) PCA applied NIRS signal Fig. 4(a)-(c)

World Academy of Science, Engineering and Technology
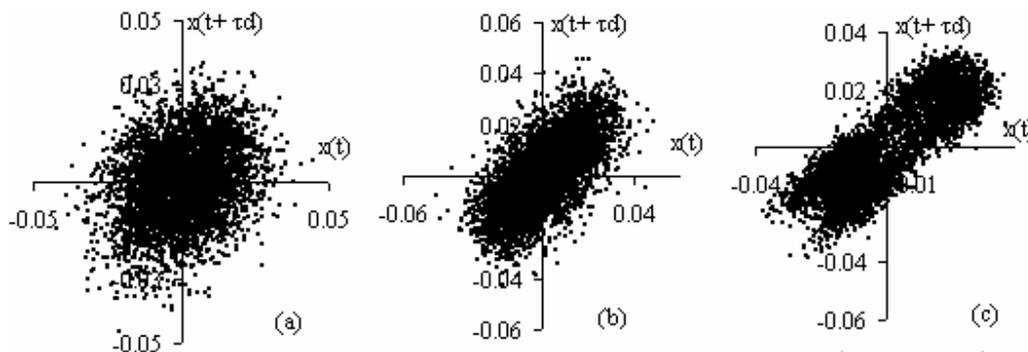International Journal of Psychological and Behavioral Sciences
Vol:2, No:3, 2008

Fig. 7 Two dimensional portrait of the PCA applied NIRS signal (a) Oxy-Hb (b) Deoxy-Hb and (c) Total-Hb concentration of imagery of left hand movement

F. Lyapunov analysis

Lyapunov exponent (λ) is a quantitative measure of the sensitive dependence on the initial conditions. They characterize the average rate of divergence of the neighboring trajectories. A chaotic system has at least one positive Lyapunov exponent. Therefore, the existence of a positive λ for almost all initial conditions in a bounded dynamical system is widely used definition of deterministic chaos. To discriminate between chaotic dynamics and periodic signals, Lyapunov exponent (λ) is often used. Due to the great interest related to the study of experimental time series in many scientific domains, a lot of methods for computing Lyapunov index for discrete time series have been developed [32]-[38]. Some methods allow computing the whole spectrum of Lyapunov exponents [33], [35], [38] from tangent maps obtained reconstructing the dynamics on a suitable *m* dimensional space. However, all these methods require large data sets. For shorter data sets, one can just determine the presence of chaos by computing only the largest Lyapunov index as in [32], [36]. The first successful algorithm for calculating the entire spectrum of Lyapunov exponent is discussed in the following [33]-[34]. The current approach is principally based on the work of Sano and Sawada [35]. Let us consider a general *m*-dimensional discrete time dynamical system,

$$\mathbf{X}_{i+1} = F(\mathbf{X}_i), \ \mathbf{X}_i \in \mathbf{R}^m \tag{10}$$

Where $\mathbf{X}_i$ is a state of the system and $F : \mathbf{R}^m \to \mathbf{R}^m$ is a m-dimensional mapping. Considering the infinitesimal small displacement at $\mathbf{X}_i$ be $\delta\mathbf{X}_i$. Then, there holds:

$$\mathbf{X}_{i+1} + \delta\mathbf{X}_{i+1} = F(\mathbf{X}_i + \delta\mathbf{X}_i) \tag{11}$$

By forming the Taylor expansion and applying the linear approximation, the following mapping is obtained for the small displacement $\delta\mathbf{X}_i$ at $\mathbf{X}_i$:

$$\delta\mathbf{X}_{i+1} = DF(\mathbf{X}_i)\delta\mathbf{X}_i \tag{12}$$

where $DF(X_i)$ is the Jacobian matrix of F at point X_i. The mapping is a time dependent linear mapping. Defining $\delta\mathbf{X}_0$ as the initial value and executing N time mappings by DF, there results:

$$\delta\mathbf{X}_N = DF(\mathbf{X}_{N-1})DF(\mathbf{X}_{N-2}) \dots DF(\mathbf{X}_0)\delta\mathbf{X}_0 \tag{13}$$

The Jocobian matrix DF_N at the N-th mapping is defined as:

$$DF_N = DF(\mathbf{X}_{N-1})DF(\mathbf{X}_{N-2}) \dots DF(\mathbf{X}_0) \tag{14}$$

Further a linearized map DF of Eq. (9) in the tangent space is estimated from the experimental data according to the method by Sano and Sawada [26]. Using the eigenvalues $\sigma_i(N)$, the Lyapunov spectrum λ_i (i = 1, 2 …m) is derived as followed:

$$\lambda_i = \lim_{N \to \infty} \frac{1}{N} \log|\sigma_i(N)| \tag{15}$$

The Lyapunov exponent, λ_i is defined as a divergence rate in bits per unit time (bits/sec) i.e. logarithm of base two. In the case of experimental time series, the Jacobian matrix of Eq. (9) cannot directly be used since the dynamical system of the object of measurement is unknown. The Jacobian matrix of Eq. (9) in the tangent space is estimated from the experimental data according to the method by Sano and Sawada [35]. This method was applied in many application fields such as EEG and vocal sound [5]-[8] but newly applied in NIRS signal in the research.

The Lyapunov spectrum is closely related to the fractional dimension of the associated strange attractor. The Lyapunov dimension (D_L) conjectured by Kaplan and York [39] can be calculated from the Lyapunov spectrum by the following equation.

$$D_L = j + \frac{\sum_{i=1}^{j} \lambda_i}{|\lambda_{j+1}|} \tag{16}$$

where j is the maximum integer such that the sum of the Lyapunov exponents in descending order is positive.

III. EXPERIMENTAL RESULTS

The analysis would operate on the time series of oxy-Hb, deoxy-Hb and total-Hb at C4 channel of the NIRS system of imagery of left-hand, real left movement and relax condition.

For the analysis of NIRS signal, it was started by presenting the most traditional forms of data analysis, direct inspection of the time series, and preprocessing by PCA. Then, evolved into techniques of chaos theory, which will allow a distinction on whether the irregularities in the NIRS signals are noise or possibly chaos. In the latter case, a quantitative characterization of the complexity of the dynamics is provided in terms of the Lyapunov spectrum and Lyapunov dimension D_L for time series of NIRS. In other words, the validity of nonlinear

World Academy of Science, Engineering and Technology
International Journal of Psychological and Behavioral Sciences
Vol:2, No:3, 2008

analysis in this study is verified. The results of analysis of one of the subjects at motor imagery task are shown in this paper.

The Lyapunov spectrum of the trajectory was estimated by using the algorithm proposed by Sano and Sawada method [35]. In order to get good statistics on the Lyapunov spectrum, it was analyzed for not only single run but also 1000 runs of each signal with random initial conditions and their average value and standard deviation. The convergences of Lyapunov spectrum for single run of original NIRS signal of Fig. 2(a)-(c) are shown in the left panel of Fig. 8(a)-(c). Fig. 9 (a) shows the convergence of Lyapunov dimension of that NIRS signal. The estimated largest Lyapunov exponent is ~7 bits/sec and Lyapunov dimension is ~3. The convergences of Lyapunov spectrum for single run of PCA applied NIRS signal of Fig. 4(a)-(c) are shown in the right panel of Fig. 8(a)-(c). Fig. 9 (b) shows the convergence of Lyapunov dimension of NIRS

signal. The estimated largest Lyapunov exponent is ~1.6 bits/sec and Lyapunov dimension is ~3. Table I shows the result for 1000 runs of chaotic dynamical systems of experimental original NIRS data for the Lyapunov spectrum (λ_i), Kaplan and Yorke dimension (D_L). Table II shows the result for 1000 runs of chaotic dynamical systems of experimental PCA filtered NIRS data for the Lyapunov spectrum (λ_i), Kaplan and Yorke dimension (D_L). Fig. 10 (a) and Fig. 11(a) show the largest Lyapunov exponents and Lyapunov dimension for imaginary of left hand movement of original NIRS signal of single subjects for different recording day. Fig. 10 (b) and Fig. 11(b) show that the largest Lyapunov exponents for imaginary of left hand movement of PCA applied NIRS signal of single subjects for different recording day. The total-Hb has smallest Lyapunov exponent and dimension for both signal.
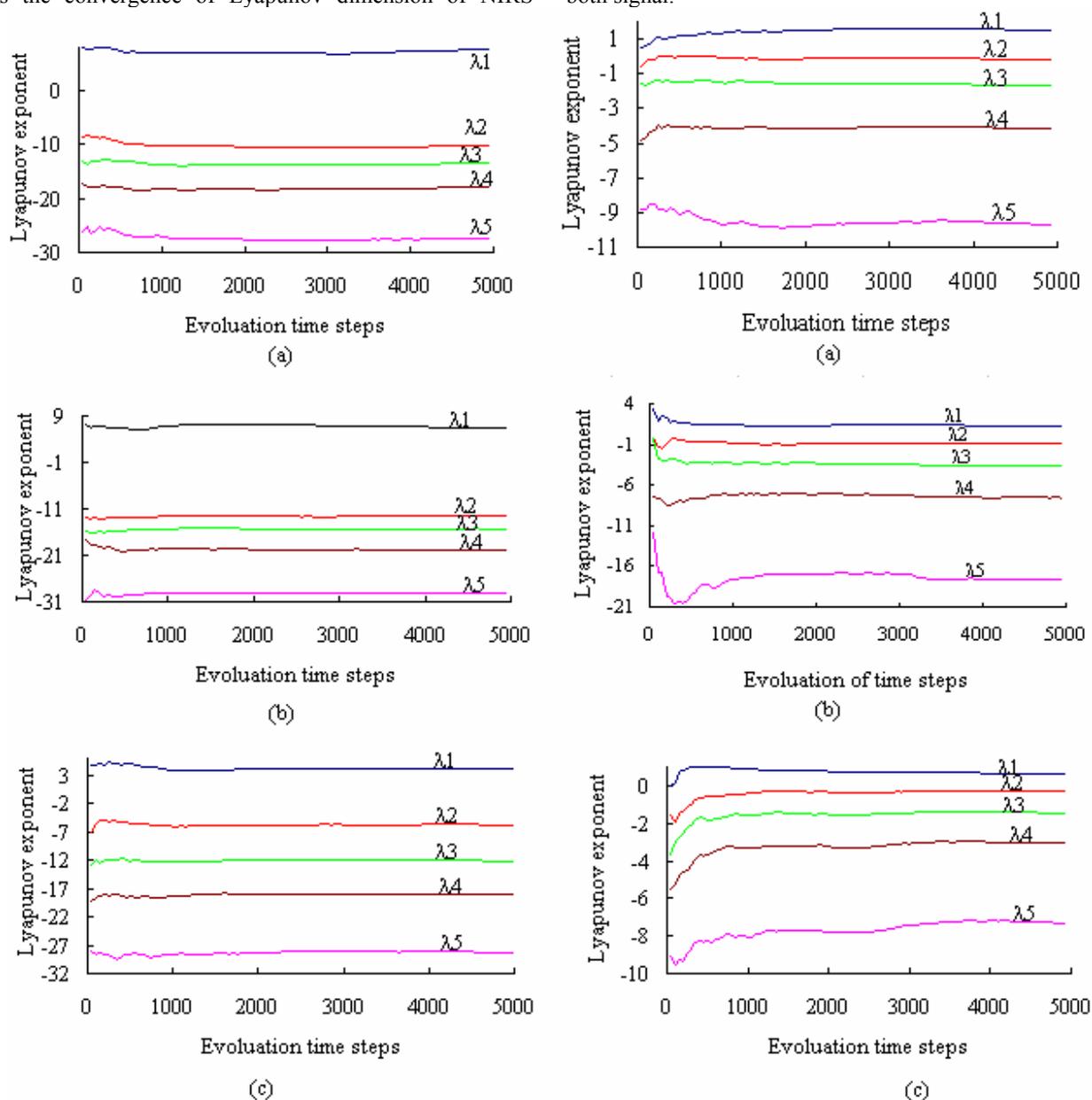

Fig. 8 Convergence of Lyapunov spectrum for single runs of original NIRS signal shown in Fig. 2(a)-(c) (left column (a)-(c)), and Convergence of Lyapunov spectrum for single runs of PCA applied NIRS signal shown in Fig. 5(a)-(c) (right column (a)-(c)).

World Academy of Science, Engineering and Technology
International Journal of Psychological and Behavioral Sciences
Vol:2, No:3, 2008

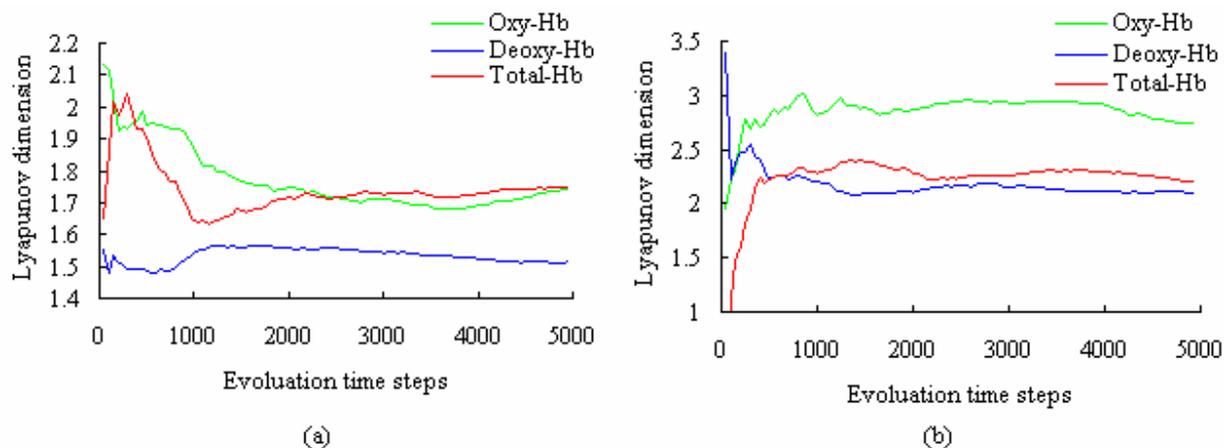(a)   (b)

Fig. 9 (a) Convergence of Lyapunov dimension for single runs of original NIRS signal shown in Fig. 2(a)-(c), and
(a)   Convergence of Lyapunov dimension for single runs of PCA applied NIRS signal shown in Fig. 5(a)-(c)

TABLE I LYAPUNOV SPECTRUM AND ESTIMATED LYAPUNOV DIMENSION FOR IMAGERY TASK OF ORIGINAL NIRS SIGNAL. THE ERROR BARS ARE CALCULATED FROM THE STANDARD DEVIATION OF 1000 RUNS

NIRS signal at C4	τ_d	m	Lyapunov Exponent (λ_i) (bit/s)	Lyapunov Dimension (D_L)
Oxy-Hb N = 24800 f_s= 40	20	5	7.2298±0.395 -10.1045±0.070 -13.389±0.074 -17.835±0.064 -27.369±0.158	1.715472±0.038
Deoxy-Hb N = 24800 f_s= 40	20	5	7.092±0.3462 -12.275±0.172 -15.067±0.192 -19.53±0.138 -29.07±0.283	1.578229±0.035
Total-Hb N = 24800 f_s= 40	15	5	4.308±0.054 -5.675±0.074 -11.964±0.123 -18.009±0.090 -28.281±0.102	1.759132±0.007

TABLE II LYAPUNOV SPECTRUM AND ESTIMATED LYAPUNOV DIMENSION FOR IMAGERY TASK OF PCA APPLIED NIRS SIGNAL. THE ERROR BARS ARE CALCULATED FROM THE STANDARD DEVIATION OF 1000 RUNS

NIRS signal at C4	τ_d	m	Lyapunov Exponent (λ_i) (bit/s)	Lyapunov Dimension (D_L)
Oxy-Hb N = 24800 f_s= 40Hz	12	5	1.536±0.0468 -0.178±0.02163 -1.721±0.0135 -4.187±0.0529 -9.648±0.1054	2.788775±0.0341
Deoxy-Hb N = 24800 f_s= 40Hz	15	5	1.063±0.1504 -1.029±0.1147 -3.649±0.1391 -8.033±0.5081 -18.88±0.9726	1.960963±0.135
Total-Hb N = 24800 f_s= 40Hz	20	5	0.605±0.0139 -0.379±0.0247 -1.468±0.018 -3.145±0.0395 -7.227±0.0626	2.153544±0.017

World Academy of Science, Engineering and Technology
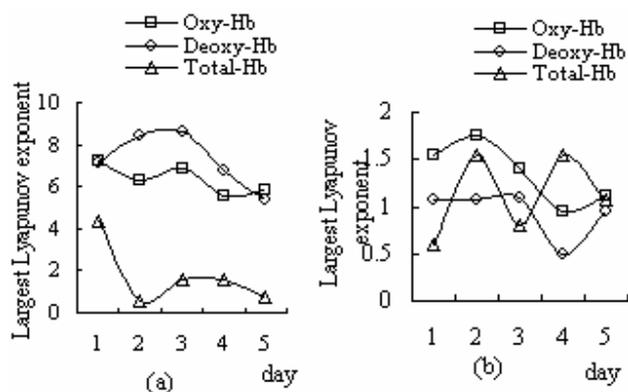International Journal of Psychological and Behavioral Sciences
Vol:2, No:3, 2008

Fig. 10 Dependent of Largest Lyapunov exponent on different date (a) original NIRS signal and (b) PCA applied NIRS signal
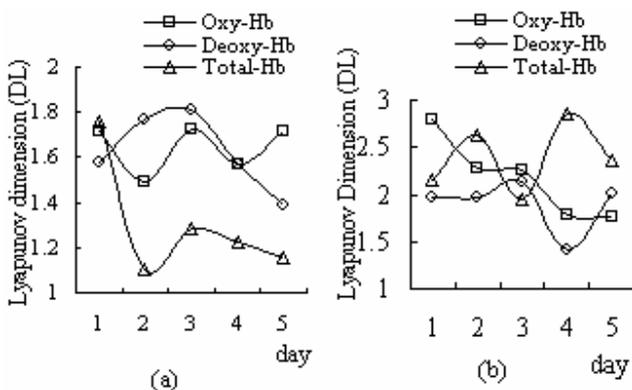

Fig. 11 Dependent of Lyapunov dimension on different date (a) original NIRS signal and (b) PCA applied NIRS signal

IV. DISCUSSIONS

In this paper, first, the NIRS signals were analyzed by PCA to ensure the signal for preprocessing of high frequency component noise. The signal was reconstructed by using largest eigenvector component and preceded for further analyzing. The existences of the chaos in the NIRS signal are verified for real and imaginary of motor movement and relax condition. The Lyapunov exponent is a measure of separation of trajectories that diverge widely from their initial close positions. The larger the exponent the more chaotic/more sensitive to the initial condition the system is.

The results from the nonlinear measures suggest that the NIRS of motor sensory cortex possesses a structure in its phase space resembling what can be found in systems with a strange attractor and thus the presence of deterministic chaos. Furthermore, largest Lyapunov exponent, λ_1 is positive ($\lambda_1 \sim 8$) for original NIRS signal of three subjects at Motor imagery in this study and λ_1 is also positive ($\lambda_1 \sim 2$) for reconstructed signal by PCA. The fractal property is verified around ($D_L \sim 2$) for original signal and ($D_L \sim 3$). Thus, it is shown that motor imaginary tasks of NIRS signal have the chaotic property. Moreover, λ_1 and D_L increased in specific tasks as shown in Table III. λ_1 has recently been used to quantify morphological

regularity ratings in the NIRS signal regardless of its level of chaos. This indicates that task performing NIRS became more complex and less regular and predictable (greater D_L) for real left hand movement than base line and imagery motor tasks of NIRS signal.

Both D_L and λ_1 were able to provide insight about reptilian NIRS features that would have remained undisclosed. These features showed small changes among different mental states. This would represent an important step in our knowledge of brain hemodynamic response; because it would demonstrate that several neural networks are able to couple with each other in a nonlinear way to produce the NIRS signal. Finally, the change of hemodynamic response for imaginary motor movement in brain activity, which was highlighted especially by Lyapunov dimension, D_L, is also a striking result that deserves further investigation to elucidate its relevance in biological signal evolution.

In conclusion, motor imagery strongly influences nonlinear of hemodynamic response. The experimental results show that NIRS signals are composed of chaos property and the attractor of NIRS is in systems with a strange attractor and thus the presence of deterministic chaos. Chaotic analysis showed that the Lyapunov exponent of brain waves increased during the imagery, and decreased during the relax condition. The present results indicated that the motor imagery promoted the neurochaos phenomenon based on the neuron activity and parasympathetic-division activity.

All the quantifiers proposed to date require considerable effort to extract their numerical value from the data. The results suggest that fractal dimension may serve as a sensitive index for quantifying dynamical changes in NIRS signals during imaginary motor tasks. Moreover, the present approach has the potential to become a useful tool to characterize the patterns of motor-related cortical activities for the classification of biological research as well as optical brain-computer interface (BCI) research [16]-[18]

TABLE III   DEPENDENT OF LARGEST LYAPUNOV EXPONENT AND LYAPUNOV DIMENSION FOR DIFFERENT TASKS OF PCA APPLIED NIRS SIGNAL. THE ERROR BARS ARE CALCULATED FROM THE STANDARD DEVIATION OF 1000 RUNS

NIRS signal at C4	Chaos parameter	Relax condition	Real Movement	Imagery Movement
Oxy-Hb N = 24800 f_s = 40Hz	λ_1	0.4438±0.0384	1.522±0.037	1.536±0.047
	D_L	1.2704±0.0254	3.449±0.067	2.789±0.034
Deoxy-Hb N = 24800 f_s = 40Hz	λ_1	0.121±0.015	1.709±0.065	1.063±0.15
	D_L	1.059±0.007	3.319±0.014	1.961±0.135
Total-Hb N = 24800 f_s = 40Hz	λ_1	0.264±0.051	0.333±0.017	0.605±0.014
	D_L	1.216±0.047	2.336±0.018	2.154±0.017

World Academy of Science, Engineering and Technology
International Journal of Psychological and Behavioral Sciences
Vol:2, No:3, 2008

REFERENCES

[1] J. Decety, "The neurophysiological basis of motor imagery", *Behavioral Brain Research,* vol. 77(1–2), pp. 45–52, 1996.

[2] G. Pfurtscheller, C. Neuper, and N. Birbaumer," Human brain-computer interface". In E. Vaadia and A. Riehle (Eds.), *Motor cortex in voluntary movements: A distributed system for distributed functions. Series: Methods and new frontiers in neuroscience,* pp. 367–401, 2005. Boca Raton, FL: CRC Press.

[3] M. Nakagawa,"*Chaos and fractals in engineering*", World Scientific, Singapore, pp. 113, 1999.

[4] M. Phothisonothai and M. Nakagawa, "EEG-Based Fractal Analysis of Different Motor Imagery Tasks using Critical Exponent Method", *International Journal of Biomedical Science*, vol. 1, no.3, pp 1306-1216, 2006.

[5] Ni Ni Soe and M. Nakagawa, "Chaos and fractal analysis of EEG signals during different imaginary motor movement tasks", *J. Phys. Soc. Jpn.*, (submitted for publication).

[6] G. Hori, K. Aihara, Y. Mizuno and Y. Okuma, "Blind source separation and chaotic analysis of EEG for judgment of brain death", *Artif. Life Robotics.*, vol. 5, no. 1, pp. 10-14, 2001.

[7] V. Vuksanović and V. Gal, "Nonlinear and chaos characteristics of heart period time series: healthy aging and postural change", *Autonomic Neuroscience: Basic and Clinical*, vol. 121, pp. 94 – 100, 2005.

[8] H. Koga and M. Nakagawa," A Chaotic Synthesis Model of Vowels ", *J. Phys. Soc. Jpn.*, vol. 72, no.3, pp. 751-761, 2003.

[9] T. J. Huppert, R. D. Hoge, S. G. Diamond, M. A. Franceschini, and D. A. Boas," A temporal comparison of BOLD, ASL, and NIRS hemodynamic responses to motor stimuli in adult human", *NeuroImage*, vol. 29, pp. 368-382, 2006.

[10] V. Y. Toronov, X. Zhang and A. G. Webb," A spatial and temporal comparison of hemodynamic signals measured using optical and functional magnetic resonance imaging during activation in human primary visual cortex", *NeuroImage*, vol. 34, pp. 1136-1148, 2007.

[11] Barbara Stuart, "*Infrared Spectroscopy: Fundamental and applications*", John Wiley and sons, 2004.

[12] C. B. Akgül, B. Sankur and A. Akin, "Extraction of cognitive activity-related waveforms from functional near-infrared spectroscopy signals", *Med. Bio. Eng. Comput.*, vol. 44, pp. 945-958, 2006

[13] R. N. Aslin, and J. Mehler," Near-infrared spectroscopy for functional studies of brain activity in human infants: promise, prospects, and challenges", *Journal of Biomedical Optics*, vol.10, no.1, pp. 011009, 2005.

[14] C. B. Akgül, B. Sankur and A. Akin," Spectral analysis of event-related hemodynamic responses in functional near infrared spectroscopy", *Journal of Computational Neuroscience*, vol. 18, pp. 67-83, 2005.

[15] M. Okamoto and I. Dan, "Functional near-infrared spectroscopy for human brain mapping of tase-related cognitive functions", *Journal of Bioscience and Bioengineering*, vol. 103, no.3, pp. 207-215, 2007.

[16] R. Sitaram, et al., "Temporal classification of multichannel near-infrared spectroscopy signals of motor imagery for developing a brain computer interface", *NeuroImage*, vol. 34, pp. 1416-1427, 2007.

[17] S. Coyle, T. Ward, and C. Markham," Brain-computer interface using a simplified functional near-infrared spectroscopy system", *Journal of Neural Engineering*, vol. 4, pp. 219-226, 2007.

[18] S. Coyle, T. Ward, C. Markham and G. McDarby," On the suitability of near-infrared (NIR) systems for next-generation brain computer interface", *Physiological Measurement*, vol. 25, pp. 815-822, 2004.

[19] D. Friedman, R. Leeb, A. Antley, M. Garau, C. Guger, C. Keinrath, A. Steed, G. Pfurtscheller, and M. Slater," Navigating virtual reality by thought: What is it like?", *Presence: Teleoperators and Virtual Environments*, vol.16 (1), pp.100-110, 2007.

[20] A. H. Nayfeh and B. Balachandran, "*Applied nonlinear dynamics: analytical, computational, and experimental methods*", New York, John Wiley and Sons, 1995.

[21] H.G. Schuster, "*Deterministic chaos: an introduction*", Weinheim, Wiley-VCH, 1989.

[22] E. Ott, "*Chaos in dynamical systems*", Cambridge, Cambridge University Press, 2002.

[23] S. H. Strogatz, "*Nonlinear dynamics and chaos*", Boston (MA), Addison-Wesley, 1994.

[24] D. T. Kaplan and L. Class,"*Understanding nonlinear dynamics*", New York, Springer, 1995.

[25] J. C. Sprott, "*Chaos and Time-Series Analysis*", Oxford University, New York, 2003.

[26] R. C. Hilborn, "*Chaos and Nonlinear Dynamics: An Introduction for Scientists and Engineers*", Oxford University, New York, 2nd ed., pp. 323, 2000.

[27] E. Ott, T. Sauer and J. Yorke, "*Coping with chaos*", John Wiley and Sons, Inc. New York, 1994.

[28] "*Handbook of chaos control*",ed. H. G. Schustetr, Wiley-VCH, Weinheim, 1999.

[29] F. Takens. "Detecting strange attractors in turbulence", *Lecture Notes in Mathematics of Dynamical Systems of Turbulence* (Springer-Verlag, Berlin, 1981), Vol. 898, pp. 365-381.

[30] A. M. Fraser and H. L. Swinney," Independent coordinates for strange attractors from mutual information", *Phys. Rev. A*, vol. 33, pp. 1134-1140, 1986.

[31] M. B. Kennel, R. Brown and H. D. I. Abarbanel," Determining embedding dimension for phase-space reconstruction using a geometrical construction", *Phys. Rev. A*, vol. 45, pp. 3403-3411, 1992.

[32] M. T. Rosenstein, J. J. Collins and C. J. De Luca, "A practical method for calculating largest Lyapunov exponents from small data sets", *Physica D*, vol. 65, pp. 117-134, 1993.

[33] I. Shimada and T. Nagashima, "A numerical approach to ergodic problem of dissipative dynamical systems", *Prog. Theor. Phys.*, Vol. 611, no.6, pp. 1605-1616, 1979. [in Japanese].

[34] A.Wolf, J.B. Swift, H.L. Swinney, and J.A. Vastano, "Determining Lyapunov exponents from a time series" *Physica D*, vol. 16, pp. 285-317, 1985.

[35] M.Sano and Y. Sawada, "Measurement of the Lyapunov spectrum from a chaotic time series", *Phys. Rev. Lett.,* vol. 55, no.10, pp. 1082-1085, 1985.

[36] S. Sato, M. Sano and Y. Sawada, "Practical methods of measuring the generalized dimension and the largest Lyapunov exponent in high dimensional chaotic systems", *Prog. Theor. Phys.*, vol. 77, no.1, pp.1-5, 1987.

[37] P. Bryant, R. Brown, and H. D. I. Abarbanel, "Lyapunov exponents from observed time series", *Phys. Rev. A*, vol. 65, pp.1523-1526, 1990.

[38] R. Brown, P. Bryant, and H. D. I. Abarbanel," Computing the Lyapunov spectrum of a dynamical system from observed time series", *Phys. Rev. A*, vol. 43, pp. 2787-2806, 1991.

[39] P. Frederickson, J. Kaplan, E. Yorke and J. Yorke, "The Lyapunov dimension of Strange Attractors", *J. Diff. Eqs.*, vol. 49, pp 185-207 ,1983.

[40] P. Gruber, et.at., "Denoising using local ICA and a generalized eigendecomposition with time-delayed signals", In *LNCS 3195, Proc. ICA' 2004*, pp 993–1000, Granada, 2004.